


## Article

# A Novel Method for Accurate Determination of the Output Voltage Ripple of DC Converters in All Operating Modes

Nicolae Lucanu , Mihai Lucanu, Ovidiu Ursaru and Cristian Aghion

Faculty of Electronics, Telecommunications and Information Technology, “Gheorghe Asachi” Technical University, 700506 Iasi, Romania; mlucanu@etti.tuiasi.ro (M.L.); ovidiu@etti.tuiasi.ro (O.U.); aghion@etti.tuiasi.ro (C.A.)

\* Correspondence: nlucanu@etti.tuiasi.ro

**Abstract:** This paper introduces a novel, high-accuracy method for determining the output voltage ripple in DC–DC converters. For the buck converter, the proposed approach enables accurate ripple estimation even under discontinuous conduction mode (DCM) operation. In the case of boost and buck–boost converters, this method not only facilitates ripple calculation in DCM but also enhances accuracy in continuous conduction mode (CCM), particularly near the transition boundary between CCM and DCM. The validity of the proposed method has been confirmed through both simulations and experimental measurements, with excellent agreement observed among theoretical, simulated, and experimental results.

**Keywords:** DC–DC converter; output voltage ripple; normalized ripple

## 1. Introduction

The output voltage ripple is a critical parameter in the design and performance of DC–DC converters, as it directly influences the required value of the output capacitance connected in parallel with the load. Existing analytical expressions for estimating the ripple, normalized to the average output voltage, have primarily been developed under the assumption of continuous conduction mode (CCM) operation [1–4]. However, for boost and buck–boost converters, these expressions require refinement even in CCM when the duty cycle of the transistor’s PWM control signals approaches the boundary between CCM and discontinuous conduction mode (DCM).

In switched-mode DC power supplies where output voltage and load current vary over wide ranges during operation, converters inevitably operate in both CCM and DCM regimes [5–11]. Notably, power supplies based on buck–boost topologies—both isolated and non-isolated—are frequently designed to operate in DCM, particularly when controlled via peak current mode without slope compensation, due to the reduced dependence of output voltage on input voltage in this mode [12–17]. To optimize performance under such conditions, accurate analytical relations are required for predicting output voltage ripple in DCM.

The output voltage ripple of ideal buck, boost, and buck–boost converters has been examined in references [18–20]. In these studies, the derivation of ripple calculation formulas was based on the utilization of equivalent circuit models and an analysis of energy transfer mechanisms.

The various operating modes, which correspond to distinct ripple calculation relationships, have been classified according to the inductance values of the converters. These modes are characterized through graphical representations, thereby complicating the practical application of the methodologies.



Academic Editor: Raffaele Giordano

Received: 30 April 2025

Revised: 2 June 2025

Accepted: 7 June 2025

Published: 12 June 2025

**Citation:** Lucanu, N.; Lucanu, M.; Ursaru, O.; Aghion, C. A Novel Method for Accurate Determination of the Output Voltage Ripple of DC Converters in All Operating Modes. *Electronics* **2025**, *14*, 2406. <https://doi.org/10.3390/electronics14122406>

**Copyright:** © 2025 by the authors. Licensee MDPI, Basel, Switzerland. This article is an open access article distributed under the terms and conditions of the Creative Commons Attribution (CC BY) license (<https://creativecommons.org/licenses/by/4.0/>).

In this study, a novel approach is employed to derive the normalized relationships between output voltage ripple and average output voltage for buck, boost, and buck–boost converters. These relationships are obtained by analyzing the waveform of the output capacitor current.

This paper derives such expressions for buck, boost, and buck–boost converters. Additionally, for boost and buck–boost topologies, improved formulas are presented for ripple estimation in CCM operation near the boundary with DCM.

In the proposed approach, the delineation of the applicability domains for the various relationships is performed using an adimensional parameter, as introduced in [1]. For all converter types, the critical boundary values separating these domains depend solely on the duty cycle of the PWM control signals. This simplification facilitates the calculations and enables a more comprehensive analysis of the impact of the converter component values on the magnitude of the normalized output voltage ripple.

The proposed relationships have been validated through both simulation and experimental testing, demonstrating strong agreement between theoretical predictions and measured results.

## 2. Peak-To-Peak Voltage Ripple at the Buck Converter Output

Figure 1 illustrates the schematic of a buck converter constructed using a transistor and a diode.

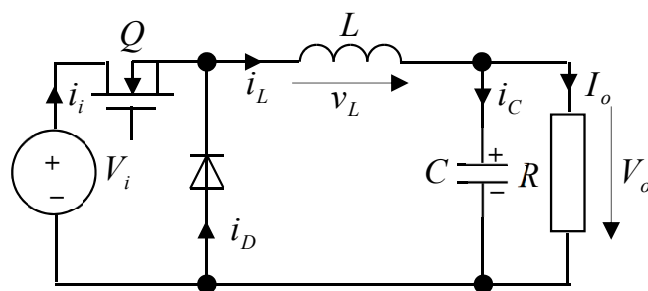


**Figure 1.** Schematic of the buck converter with a transistor and a diode.

The condition for the operation of the converter in CCM is [1,3].

$$K = \frac{2Lf}{R} \geq 1 - D \quad (1)$$

In (1),  $K$  represents the dimensionless quantity that defines the conduction mode,  $L$  is the converter inductance,  $f$  is the switching frequency,  $R$  is the load resistance, and  $D$  is the duty cycle of the transistor control MID pulses.

When operating in CCM, the relationship for calculating the ripple normalized to the average value of the output voltage of the ideal buck converter is [1,3]

$$\frac{\Delta v_o}{V_o} = \frac{1 - D}{8f^2LC} \quad (2)$$

In (2),  $\Delta v_o$  represents the peak-to-peak ripple of the output voltage,  $V_o$  is the average value of this voltage, and  $C$  is the parallel capacitance of the load resistance.

In the ideal converter, the transistor and diode are considered ideal switches with zero on-resistance, infinite off-resistance, and zero switching times. The other circuit components are considered lossless. The condition for the operation of the buck converter in DCM is [1,3]

$$K = \frac{2Lf}{R} \leq 1 - D \quad (3)$$

Figure 2 presents the inductor current  $i_L(t)$  and capacitor current  $i_C(t)$  waveforms corresponding to the ideal buck converter operating in DCM. The waveform  $i_C(t)$  is plotted based on the equation

$$i_C(t) = i_L(t) - I_o = i_L(t) - I_L \quad (4)$$

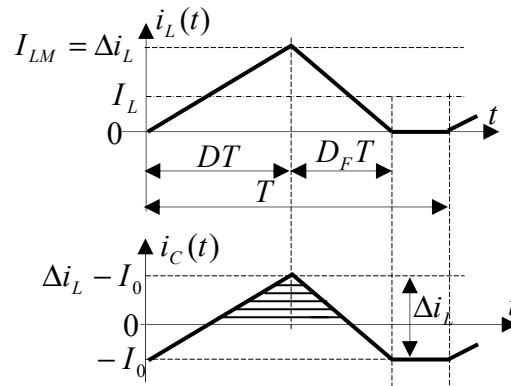


**Figure 2.** Inductor current  $i_L(t)$  and capacitor current  $i_C(t)$  waveforms of the ideal buck converter.

In this figure, the flyback duty cycle (of the diode) is denoted by  $D_F$ ,  $I_o$  represents the load current assumed as constant ( $I_o = V_o/R$ ), and  $I_L$  is the average value of the inductor current ( $I_o = I_L$ ).

Since the average value of the current through the capacitor is equal to zero, the following relation can be written as

$$(\Delta i_L)(D + D_F)T = 2I_o T \quad (5)$$

In (5),  $\Delta i_L$  represents the peak-to-peak ripple of the inductor current, and  $T = 1/f$  is the switching period. The following relations [1,3,21] are valid for the DCM operating of the buck converter:

$$\Delta i_L = \frac{D(V_i - V_o)}{Lf}, \quad I_L = \frac{V_o}{R}, \quad \frac{\Delta i_L}{I_L} = \frac{DR}{Lf} \frac{V_i - V_o}{V_o} = \frac{2D}{K} \left( \frac{1}{M} - 1 \right) \quad (6)$$

where  $M$  is the conversion ratio of the DCM buck converter given by [1,21–23]

$$M = \frac{V_o}{V_i} = \frac{2}{1 + \sqrt{1 + \frac{4K}{D^2}}} \quad (7)$$

From (6) and (7), the following equation results:

$$\frac{\Delta i_L}{I_L} = \frac{\Delta i_L}{I_o} = \frac{4}{D + \sqrt{D^2 + 4K}} \quad (8)$$

The electrical charge  $\Delta q$  stored in the capacitor for the duration  $i_C(t) \geq 0$  is given by

$$\Delta q = C\Delta v_o = \text{hatched area} = \left( 1 - \frac{I_o}{\Delta i_L} \right)^2 \frac{\Delta i_L}{2} (D + D_F)T \quad (9)$$

Inserting the expression  $D + D_F$  from (5) into (9), we obtain

$$\frac{\Delta v_o}{V_o} = \frac{1}{fRC} \left( 1 - \frac{I_o}{\Delta i_L} \right)^2 = \frac{1}{fRC} \left( 1 - \frac{I_L}{\Delta i_L} \right)^2 \quad (10)$$

In (10),  $I_L / \Delta i_L$  is replaced with the expression from (8), and the following expression is obtained for the calculation of the peak-to-peak ripple relative to the average value of the output voltage for the DCM operating buck converter:

$$\frac{\Delta v_o}{V_o} = \frac{1}{16fRC} (4 - D - \sqrt{D^2 + 4K})^2 \quad (11)$$

The following relations are valid at the border between DCM and CCM operating modes:

$$K = 1 - D, R = \frac{2fL}{1 - D} \quad (12)$$

For a first verification of (11), the relations in (12) are introduced into (11), and the expression (2) is correctly obtained. Over the entire range of variation of the duty cycle  $D \in [0, 1]$ , the peak-to-peak ripple normalized to the average value of the output voltage of the ideal buck converter is expressed by

$$\frac{\Delta v_o}{V_o} = \begin{cases} \frac{1-D}{8f^2LC} & \text{for } K \geq 1 - D \quad \text{CCM} \\ \frac{(4-D-\sqrt{D^2+4K})^2}{16fRC} & \text{for } K \leq 1 - D \quad \text{DCM} \end{cases} \quad (13)$$

The procedure for deriving the normalized peak-to-peak ripple of the buck converter's output voltage, given the input voltage  $V_i$ , output voltage  $V_o$ , load resistance  $R$ , inductance  $L$ , and output capacitance  $C$ , is outlined as follows:

(a) Assuming the converter operates in CCM, the voltage conversion ratio  $M$ , duty cycle  $D$ , and the dimensionless parameter  $K$  are calculated using the following relations:

$$M = \frac{V_o}{V_i}, D = M, K = \frac{2Lf}{R} \quad (14)$$

Using these computed values, the applicable inequality—either (1) or (3)—is checked to determine whether the converter operates in CCM or in DCM.

(b) If CCM is confirmed, the peak-to-peak ripple of the output voltage is obtained from Equation (2).

(c) If DCM conditions are met, the following steps are performed:

-The duty cycle is calculated with the following relationship derived from (7):

$$D = M \sqrt{\frac{K}{1 - M}} \quad (15)$$

-The ripple of the output voltage is then calculated using (11).

To calculate the normalized peak-to-peak output voltage ripple of the buck converter, given the known parameters input voltage  $V_i$ , duty cycle  $D$ , load resistance  $R$ , inductance  $L$ , and output capacitance  $C$ , the dimensionless quantity  $K$  is computed, and (13) is employed.

The converter output voltage is determined from the value of the conversion ratio  $M$ , which in CCM is calculated with (14) and in DCM with (7).

### 3. Peak-To-Peak Voltage Ripple at the Boost Converter Output

Figure 3 shows the schematic of a boost converter implemented using a transistor and a diode. For an ideal converter operating in continuous conduction mode (CCM), assuming that the output capacitor discharges exclusively during the transistor's conduction interval (on time), the peak-to-peak voltage ripple, normalized to the average output voltage, is expressed as [21]

$$\frac{\Delta v_o}{V_o} = \frac{D}{fRC} \quad (16)$$

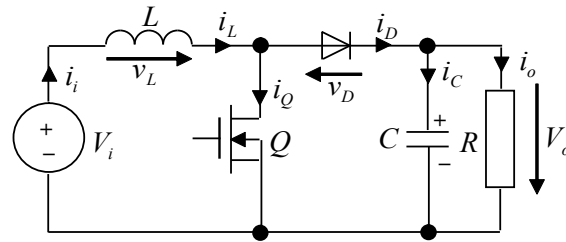


**Figure 3.** Schematic of the boost converter with a MOS transistor and a diode.

In practice, this relationship is correct only if the following inequality is verified:

$$K = \frac{2Lf}{R} \geq (1 - D)^2 \quad (17)$$

Under the condition

$$D(1 - D)^2 \leq K < (1 - D)^2 \quad (18)$$

the converter will still work in CCM, but the waveforms of the currents through the inductor and through the capacitor are those from Figure 4. The capacitor will also discharge towards the end of the duration  $(1 - D)T$  corresponding to the off interval when the transistor is blocked; therefore, (16) can no longer be used.

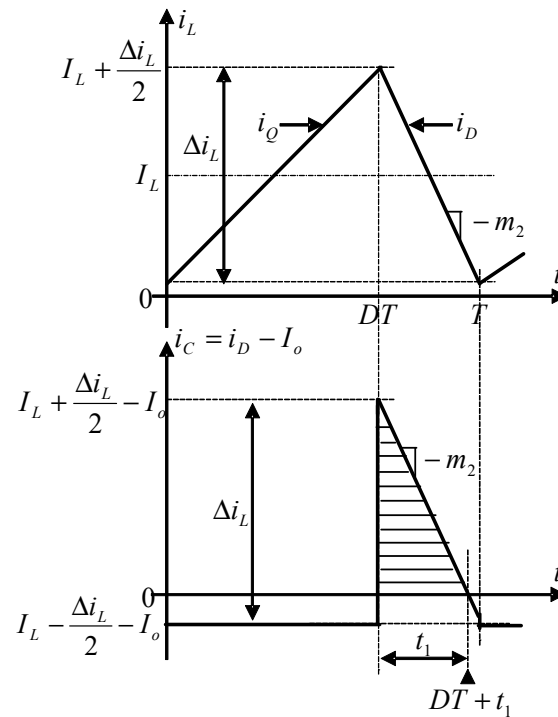


**Figure 4.** Waveforms of currents  $i_L$  and  $i_C$  for  $D(1 - D)^2 \leq K \leq (1 - D)^2$ .

The duration  $t_1$  for the capacitor to charge ( $i_C \geq 0$ ) is given by

$$t_1 = \frac{1}{m_2} \left( I_L + \frac{1}{2} \Delta i_L - I_o \right) \quad (19)$$

In the above equation,  $I_L$  and  $\Delta i_L$  represent the average value and the peak-to-peak ripple of the current through the inductor, respectively.  $I_o$  denotes the load current, which is assumed to be constant, and  $-m_2$  is the slope of the  $i_L$  current during off time.

The  $i_C$  capacitor current waveform in Figure 4 is obtained under the condition

$$t_1 = \frac{1}{m_2} \left( I_L + \frac{1}{2} \Delta i_L - I_o \right) \leq t_{off} = (1 - D)T \quad (20)$$

For the boost converter working in CCM, the following relations [1,3,21] are valid:

$$I_L = \frac{I_o}{1 - D}, \quad \Delta i_L = \frac{DV_i}{Lf}, \quad m_2 = \frac{V_o - V_i}{L}, \quad \frac{V_o}{V_i} = \frac{1}{1 - D} \quad (21)$$

By introducing (21) into (20) and taking into account that the converter operates in CCM, the condition in (18) is obtained.

From Figure 4 we obtain the following:

$$\text{hatched area} = C \Delta V_o = \frac{1}{2m_2} \left( I_L + \frac{1}{2} \Delta i_L - I_o \right)^2 \quad (22)$$

By introducing (21) in (22), the following expression of the peak-to-peak ripple normalized to the average value of the output voltage of the boost converter is obtained when the inequalities (18) are respected:

$$\frac{\Delta v_o}{V_o} = \frac{D [K + (1 - D)^2]^2}{8LCf^2(1 - D)^2} \quad (23)$$

The following relation exists for  $t_1 = t_{off} = (1 - D)T$ :

$$K = (1 - D)^2 \quad (24)$$

By introducing (24) into (23), the expression for the peak-to-peak ripple normal to the average value of the output voltage from (16) is correctly obtained.

The ratio of  $\Delta v_{o(23)}$ , which is the peak-to-peak ripple of the output voltage deduced from (23), and  $\Delta v_{o(16)}$ , which is the peak-to-peak ripple of the output voltage deduced from Equation (16), is

$$\frac{\Delta v_{o(23)}}{\Delta v_{o(16)}} = \frac{[K + (1 - D)^2]^2}{4K(1 - D)^2} \quad (25)$$

The maximum of this ratio is obtained for  $K = D(1 - D)^2$  and corresponds to the boundary between CCM and DCM, and is given as follows:

$$\left[ \frac{\Delta v_{o(23)}}{\Delta v_{o(16)}} \right]_{(\max)} = \frac{(D + 1)^2}{4D} \quad (26)$$

This ratio evaluates the difference between the normalized ripples given by (16) and (23). From (26), the Table 1 is obtained.

**Table 1.** Peak-to-peak ripple ratio given by (23) and (16) corresponding to CCM.

D	0.3	0.4	0.5	0.6
$\Delta v_{o(23)} / \Delta v_{o(16)}$	1.408	1.225	1.125	1.066

The result is that if the transition from CCM to MCD is carried out with a duty cycle  $D \leq 0.5$ , then the errors that occur if (23) is not used instead of (16) can become important.

The condition for the operation of the boost converter in DCM is given by [1,3,22]

$$K = \frac{2Lf}{R} \leq D(1-D)^2 \quad (27)$$

The waveforms of the currents through the inductor and the capacitor are shown in Figure 5.

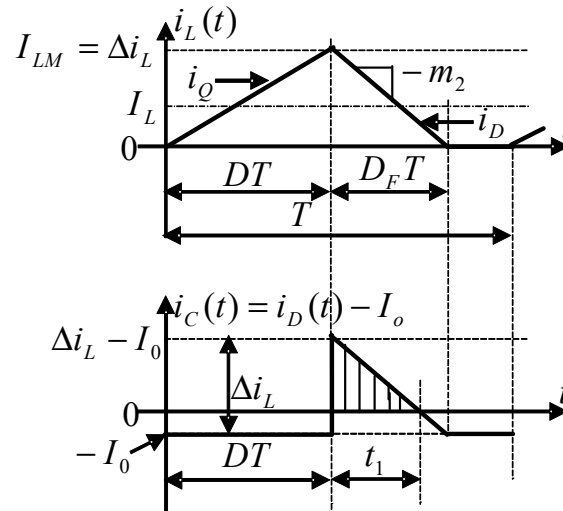


**Figure 5.** Waveforms of inductor and capacitor currents during the operation of the boost converter in DCM.

The waveform of the current through the capacitor is plotted based on the following relation:

$$i_C(t) = i_D(t) - I_o \quad (28)$$

The duration  $t_1$  for the capacitor to charge ( $i_C \geq 0$ ) is given by

$$t_1 = \frac{1}{m_2} (\Delta i_L - I_o) \quad (29)$$

In addition, we obtain

$$\text{hatched area} = C \Delta V_o = \frac{1}{2m_2} (\Delta i_L - I_o)^2 \quad (30)$$

For the boost converter working in DCM, the following relations [1–3] are valid:

$$\Delta i_L = \frac{DV_i}{Lf}, \quad m_2 = \frac{V_o - V_i}{L}, \quad M = \frac{V_o}{V_i} = \frac{1}{2} \left( 1 + \sqrt{1 + \frac{4D^2}{K}} \right) \quad (31)$$

Equations (30) and (31) lead to the following expression for the peak-to-peak ripple normalized to the average value of the output voltage of the boost converter operating in DCM:

$$\frac{\Delta v_o}{V_o} = \frac{1}{16D^2 f RC} \left( 4D - K - \sqrt{K^2 + 4KD^2} \right)^2 \quad (32)$$

The following relations are valid at the border between the CCM and DCM:

$$K = D(1-D)^2, \quad R = \frac{2fL}{D(1-D)^2} \quad (33)$$

By introducing the relations of  $K$  and  $R$  from (33) into both (23) and (32), we obtain exactly the same expressions.

Over the entire range of variation of the duty cycle  $D \in [0, 1]$ , the peak-to-peak ripple normalized to the average value of the boost converter output voltage is calculated with the following relation:

$$\frac{\Delta v_o}{V_o} = \begin{cases} \frac{D}{fRC} & \text{for } K \geq (1-D)^2 \quad \text{CCM} \\ \frac{D[K+(1-D)^2]^2}{8LCf^2(1-D)^2} & \text{for } D(1-D)^2 \leq K \leq (1-D)^2 \quad \text{CCM} \\ \frac{(4D-K-\sqrt{K^2+4KD^2})^2}{16fRCD^2} & \text{for } K \leq D(1-D)^2 \quad \text{DCM} \end{cases} \quad (34)$$

The derivation of the normalized peak-to-peak ripple of the boost converter's output voltage, given the input voltage  $V_i$ , output voltage  $V_o$ , load resistance  $R$ , inductance  $L$ , and output capacitance  $C$ , is conducted according to the following procedure:

(a) Assuming the converter operates in CCM, the voltage conversion ratio  $M$ , duty cycle  $D$ , and the dimensionless parameter  $K$  are calculated using the following relations:

$$M = \frac{V_o}{V_i}, \quad D = 1 - \frac{1}{M}, \quad K = \frac{2Lf}{R} \quad (35)$$

and the determination of whether the converter operates in CCM or DCM is made by evaluating inequality (27).

(b) If the operation mode occurs in CCM and inequality (17) is satisfied, the normalized peak-to-peak ripple of the output voltage is computed using (16).

(c) If the operation mode is CCM and inequality (18) is verified, the normalized peak-to-peak ripple of the output voltage is calculated with (23).

(d) If the operation mode occurs in DCM, the following additional two steps are necessary:

-The duty cycle is calculated using the following relationship derived from (31):

$$D = \sqrt{KM(M-1)} \quad (36)$$

-The normalized peak-to-peak ripple of the output voltage is calculated using (32).

To calculate the normalized peak-to-peak output voltage ripple of the boost converter, given the known parameters input voltage  $V_i$ , duty cycle  $D$ , load resistance  $R$ , inductance  $L$ , and output capacitance  $C$ , the dimensionless quantity  $K$  is computed, and (34) is employed.

The converter output voltage is determined from the value of the conversion ratio  $M$ , which in CCM is  $1/(1-D)$ , and in DCM is given by (31).

#### 4. Peak-To-Peak Voltage Ripple at the Buck–Boost Converter Output

The schematic of the buck–boost converter with a transistor and a diode is shown in Figure 6. In continuous conduction mode (CCM) operation, the peak-to-peak ripple normalized to the average output voltage is determined using Equation (14), which is similar to the boost converter. For the buck–boost converter, this relationship is valid only if the condition specified in inequality (15) is met. If the inequality is reversed and the converter continues to operate in CCM, the  $i_C$  current waveform follows the pattern shown in Figure 4. In this case, capacitor discharge also occurs during the off time, rendering Equation (14) invalid.



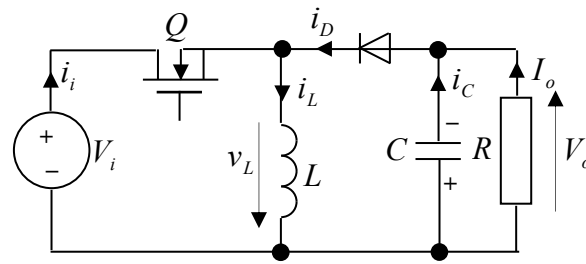


**Figure 6.** Diagram of the buck–boost converter with a transistor and a diode.

When operating in CCM, the following relations [1,3,21] apply for the buck–boost converter:

$$I_L = \frac{I_o}{1-D} = \frac{V_o}{R(1-D)} \quad , \quad \Delta i_L = \frac{DV_i}{Lf} \quad , \quad m_2 = \frac{V_o}{L} \quad , \quad M = \frac{V_o}{V_i} = \frac{D}{1-D} \quad (37)$$

Taking into account (20) and (37) and the operating condition in MCC, for the buck–boost converter, the  $i_C$  waveform from Figure 4 will be obtained if

$$(1-D)^2 \leq K \leq \frac{(1-D)^2}{D} \quad (38)$$

Under this condition, the following expression of the peak-to-peak ripple normalized to the average value of the output voltage is obtained from (22) and (37):

$$\frac{\Delta v_o}{V_o} = \frac{1}{4fRCK} \left( \frac{KD}{1-D} + 1 - D \right)^2 \quad (39)$$

If in (39) we consider the particular case

$$K = \frac{1}{D}(1-D)^2 \quad (40)$$

then Equation (16) is correctly obtained.

We denote the peak-to-peak ripple of the output voltage deduced from (39) as  $\Delta v_{o(39)}$  and the peak-to-peak ripple of the output voltage deduced from (16) as  $\Delta v_{o(16)}$ . Their ratio is given by

$$\frac{\Delta v_{o(39)}}{\Delta v_{o(16)}} = \frac{1}{4KD} \left( \frac{KD}{1-D} + 1 - D \right)^2 \quad (41)$$

The maximum of the above ratio is obtained for  $K = (1-D)^2$  and corresponds to the boundary between CCM and DCM, and is given as follows:

$$\left[ \frac{\Delta v_{o(39)}}{\Delta v_{o(16)}} \right]_{(\max)} = \frac{(D+1)^2}{4D} \quad (42)$$

The same expression was obtained for the boost converter, so Table 1 is valid in this case, too. Therefore, if the transition from CCM to DCM is made at a duty cycle  $D \leq 0.5$ , the errors that occur if (39) is not used instead of (16) can become important.

The condition for the operation of the buck–boost converter in DCM is given by [2,23] the following:

$$K = \frac{2Lf}{R} < (1-D)^2 \quad (43)$$

When operating in DCM, the waveforms of the currents through the inductor and through the capacitor are shown in Figure 5, and the following relations [1–3] can be written:

$$\Delta i_L = \frac{DV_i}{Lf}, \quad m_2 = \frac{V_o}{L}, \quad M = \frac{V_o}{V_i} = \frac{D}{\sqrt{K}} \quad (44)$$

The following expression for the peak-to-peak ripple normalized to the average value of the output voltage is obtained from (30) and (44):

$$\frac{\Delta v_o}{V_o} = \frac{1}{4fRC} (2 - \sqrt{K})^2 \quad (45)$$

For  $K = (1 - D)^2$ , the expressions in (39) and (45) coincide correctly.

The exact relationship for determining the peak-to-peak ripple normalized to the average value of the output voltage of the ideal buck–boost converter over the entire range of variation of the duty cycle  $D \in [0, 1]$  is the following:

$$\frac{\Delta v_o}{V_o} = \begin{cases} \frac{D}{fRC} & \text{for } K \geq \frac{(1-D)^2}{D} \quad \text{CCM} \\ \frac{1}{8LCf^2} \left( \frac{KD}{1-D} + 1 - D \right)^2 & \text{for } (1-D)^2 \leq K \leq \frac{1}{D}(1-D)^2 \quad \text{CCM} \\ \frac{(2-\sqrt{K})^2}{4fRC} & \text{for } K \leq (1-D)^2 \quad \text{DCM} \end{cases} \quad (46)$$

It can be observed that when the buck–boost converter operates in DCM, the peak-to-peak ripple normalized to the average output voltage is independent of the duty cycle and depends solely on the load resistance.

The calculation of the normalized peak-to-peak ripple of the buck–boost converter's output voltage, given the input voltage  $V_i$ , output voltage  $V_o$ , load resistance  $R$ , inductance  $L$ , and output capacitance  $C$ , is conducted according to the following procedure:

(a) Assuming the converter operates in CCM, the voltage conversion ratio  $M$ , duty cycle  $D$ , and the dimensionless parameter  $K$  are calculated using the following relations:

$$M = \frac{V_o}{V_i}, \quad D = 1 + \frac{1}{M}, \quad K = \frac{2Lf}{R} \quad (47)$$

The determination of whether the converter operates in CCM or DCM is made by evaluating inequality (43).

(b) If the operation mode occurs in CCM and inequality (38) is not satisfied, the normalized peak-to-peak ripple of the output voltage is computed using (16).

(c) If the operation mode is CCM and inequality (38) is verified, the normalized peak-to-peak ripple of the output voltage is calculated with (39).

(d) If the operation mode occurs in DCM, the normalized peak-to-peak ripple of the output voltage is calculated with (45).

To calculate the normalized peak-to-peak output voltage ripple of the buck–boost converter, given the known parameters input voltage  $V_i$ , duty cycle  $D$ , load resistance  $R$ , inductance  $L$ , and output capacitance  $C$ , the dimensionless quantity  $K$  is first calculated, and then (46) is applied.

The converter output voltage is determined from the value of the conversion ratio  $M$ , which in CCM is  $D/(1 - D)$ , and in DCM is given by (44).

## 5. Simulation and Experimental Verification of the Novel Expressions for the Peak-to-Peak Ripple Normalized to the Average Value of the Output Voltage

Switching power supplies are usually stabilized. In the simulated and experimentally verified converters, a constant output voltage  $V_o = 10V$  was chosen. For this, the input

voltage was modified accordingly for each converter depending on the duty cycle  $D$ . All tested converters have a switching frequency of 100 KHz.

The buck converter parameters were chosen so that at  $D = 0.6$ , it would work on the border between CCM and DCM. The other values used for the duty cycle are 0.5, 0.4, and 0.3. The load resistance is  $R = 1 \Omega$  (the power dissipated on the load resistance is 100 W), and the load parallel capacitor is  $C = 370 \mu\text{F}$ .

The characteristic values of the tested buck converter are shown in Table 2.

**Table 2.** Characteristic values of the tested buck converter.

Converter Type	$V_o$	$L$	$C$	$f$	$R$
Buck	10 V	2 $\mu\text{H}$	370 $\mu\text{F}$	100 KHz	1 $\Omega$

Simulations were conducted utilizing the OrCAD Cadence Release 9.2 software, with circuit elements sourced from the PSPICE component libraries. Table 3 lists the components used as the basis for both the simulation and practical implementation of the three converters: buck, boost, and buck–boost.

**Table 3.** Values of components used in the simulation and in practical implementation.

Device	Simulation (Orcad PSpice)	Practical Implementation
Transistor	IRF640	IRF3205
Diode	MBR8045	SBL3040PT
Capacitor	Library model (ideal)	$37 \times 10 \mu\text{F}$ (GRM32ER7YA106KA12)
Inductor	Library model (ideal)	Epcos P2323 18265C
Control	Library model ( $V_{\text{pulse}}$ )	Microcontroller Arduino Uno (+driver circuit with galvanic isolation HCPL3180)
Power supply	Library model (ideal)	ZHAOXIN DC Power Supply KXN-6020D
Oscilloscope	Library model (ideal)	MetrixScopiX OX7042-C 40 MHz, 1 GS/s
Load	Library model (ideal)	Electronic Load EA-EL 3080-60 B 0–80 V 0–400 W
Current probe	Library model (ideal)	Clamp on probe Rigol RP1003C, 50 MHz, 30 A

Figure 7a,b present the waveforms of the output voltage  $v_o$  and inductor current  $i_L$  obtained for the buck converter by simulation and by experimental tests, respectively, when operating with a duty cycle  $D = 0.3$ . The same waveforms are given in Figure 8a,b for  $D = 0.4$ , in Figure 9a,b for  $D = 0.5$ , and in Figure 10a,b for  $D = 0.6$ .

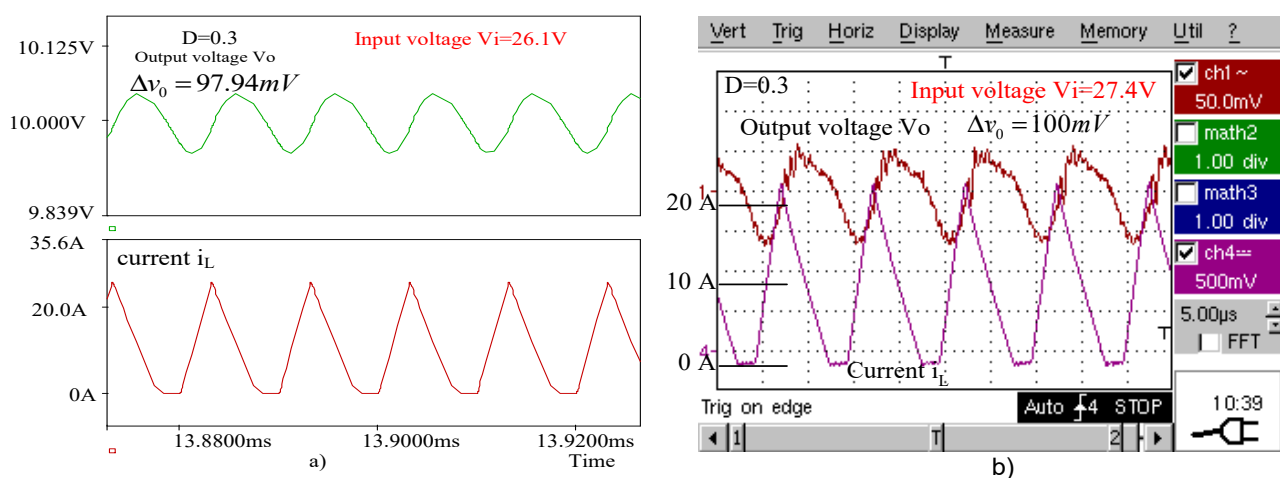


**Figure 7.** (a) Simulated waveforms of the buck converter for  $D = 0.3$ . (b) Experimental waveforms of the buck converter for  $D = 0.3$ .

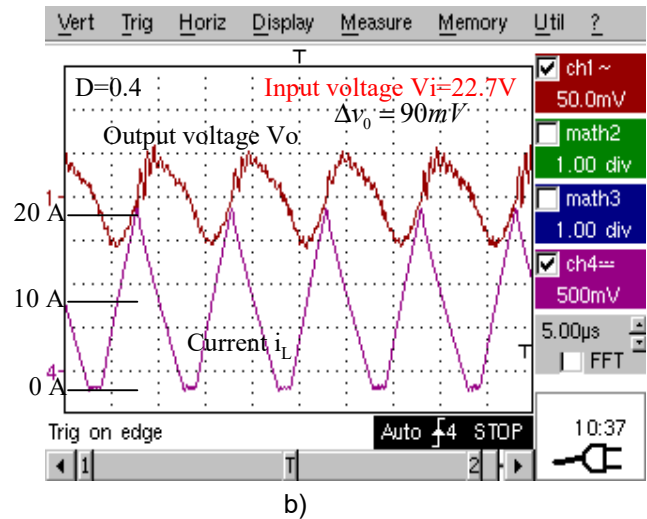
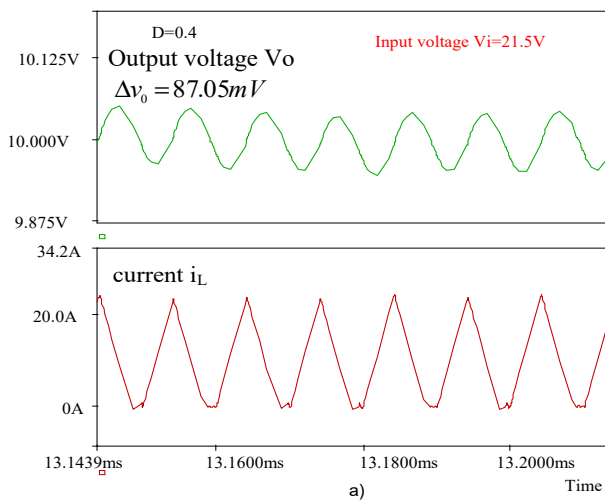


**Figure 8.** (a) Simulated waveforms of the buck converter for  $D = 0.4$ . (b) Experimental waveforms of the buck converter for  $D = 0.4$ .

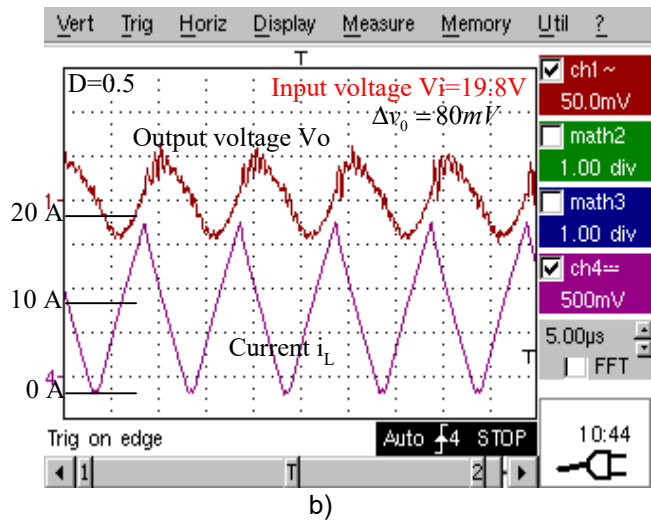
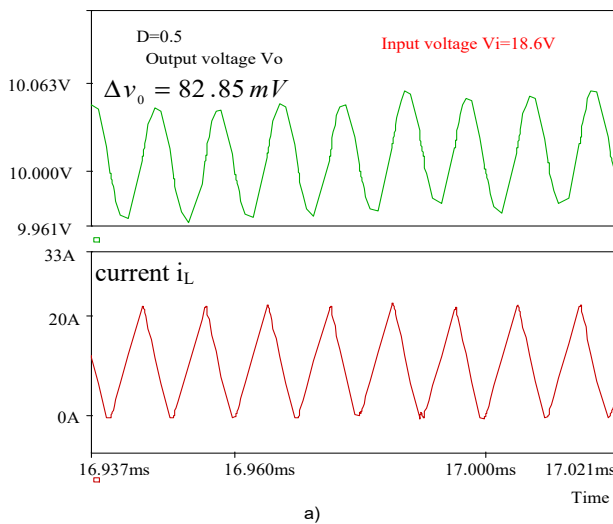


**Figure 9.** (a) Simulated waveforms of the buck converter for  $D = 0.5$ . (b) Experimental waveforms of the buck converter for  $D = 0.5$ .

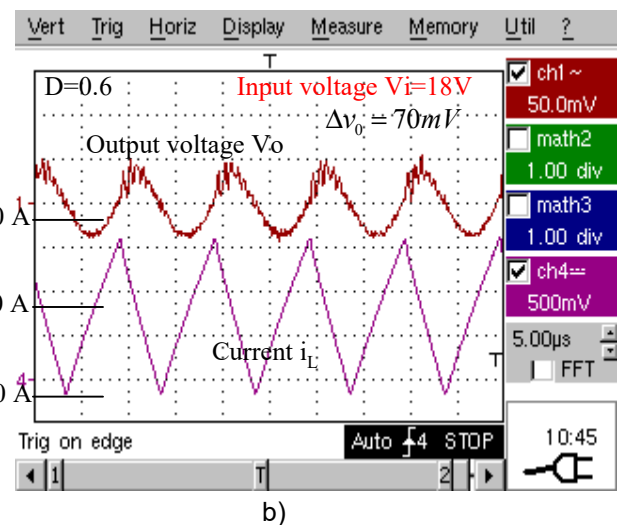
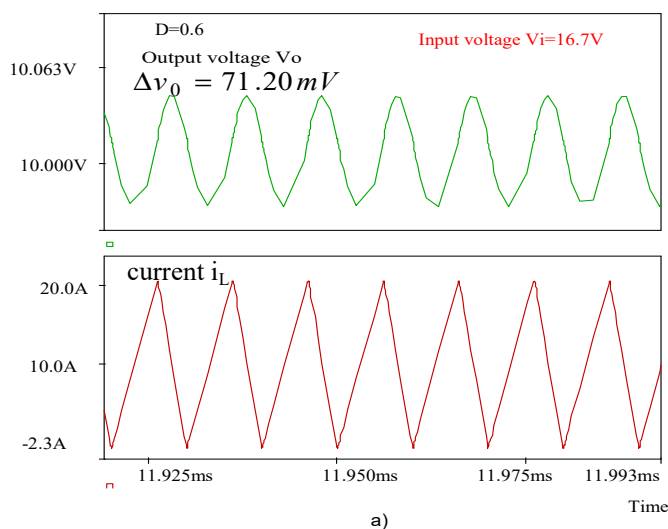


**Figure 10.** (a) Simulated waveforms of the buck converter for  $D = 0.6$ . (b) Experimental waveforms of the buck converter for  $D = 0.6$ .

The peak-to-peak voltage ripples of the buck converter output are presented in Table 4. The experimental values are compared with those calculated using the novel expressions and with the simulated ones.

**Table 4.** Peak-to-peak voltage ripples at the buck converter output.

Duty Cycle	30%	40%	50%	60%
$\Delta V_o$ experiment	100 mV	90 mV	80 mV	70 mV
$\Delta V_o$ calculated	97.29 mV	87.299 mV	77.347 mV	67.567 mV
$\Delta V_o$ simulated	97.94 mV	87.05 mV	82.85 mV	71.2 mV

The boost and buck–boost converters that were simulated and experimentally tested had the same characteristic values as the buck converter except that their load resistance was  $R = 5 \Omega$ , corresponding to a power of 20 W, as presented in Table 5.

**Table 5.** Characteristic values of the tested boost and buck–boost converters.

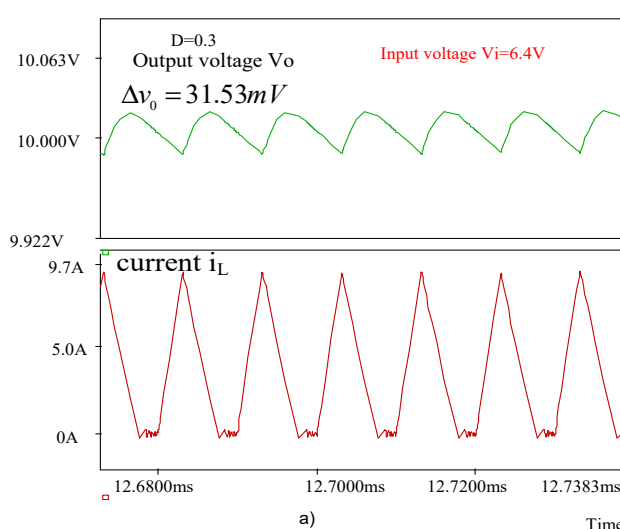
Converter Type	$V_o$	$L$	$C$	$f$	$R$
Buck	10 V	2 $\mu$ H	370 $\mu$ F	100 KHz	5 $\Omega$

Figure 11a,b present the waveforms of the output voltage  $v_o$  and inductor current  $i_L$  obtained for the boost converter by simulation and by experimental tests, respectively, when operating with a duty cycle  $D = 0.3$ . The same waveforms are given in Figure 12a,b for  $D = 0.4$ , in Figure 13a,b for  $D = 0.5$ , and in Figure 14a,b for  $D = 0.6$ .

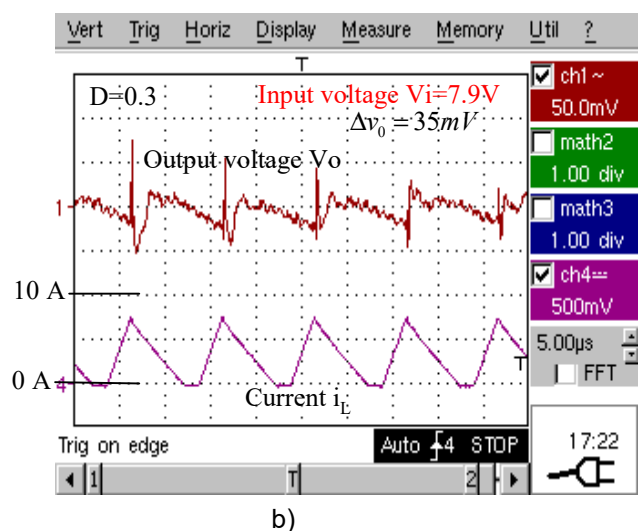
Table 6 compares the peak-to-peak voltage ripples of the boost converter experimentally obtained with those computed using the novel expressions and with the simulated ones.

**Table 6.** Peak-to-peak voltage ripples at the boost converter output.

Duty Cycle	30%	40%	50%	60%
$\Delta V_o$ experiment	35 mV	37 mV	39 mV	42 mV
$\Delta V_o$ calculated	32.632 mV	34.594 mV	35.73 mV	36.46 mV
$\Delta V_o$ simulated	31.53 mV	32.952 mV	33.3 mV	35.75 mV



a)



b)

**Figure 11.** (a) Simulated waveforms of the boost converter for  $D = 0.3$ . (b) Experimental waveforms of the boost converter for  $D = 0.3$ .

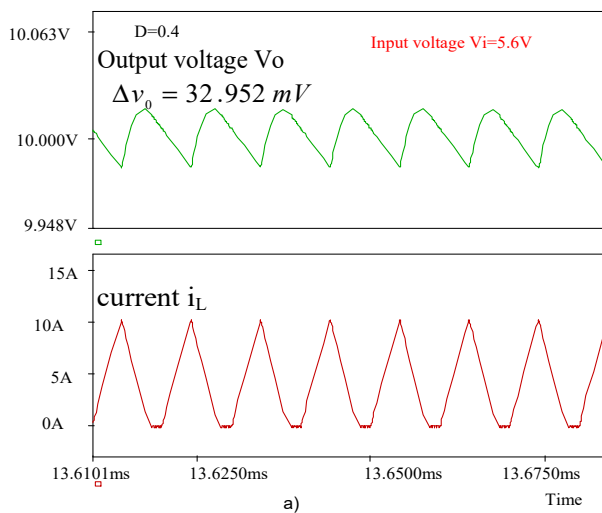


**Figure 12.** (a) Simulated waveforms of the boost converter for  $D = 0.4$ . (b) Experimental waveforms of the boost converter for  $D = 0.4$ .

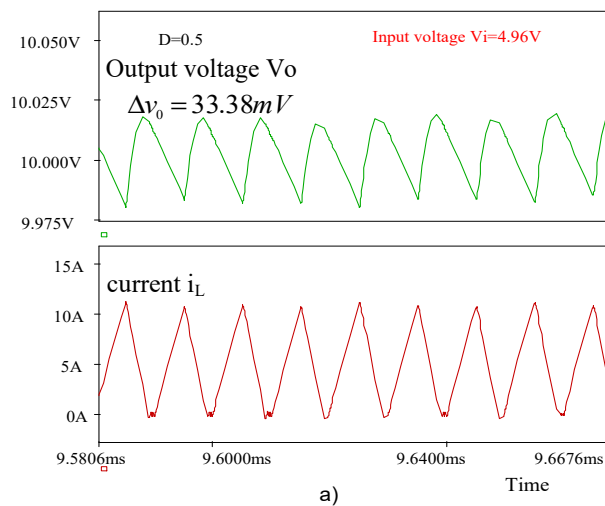
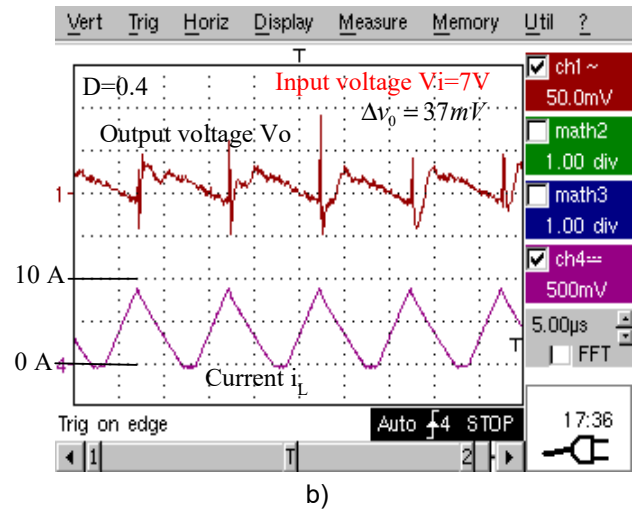


**Figure 13.** (a). Simulated waveforms of the boost converter for  $D = 0.5$ . (b) Experimental waveforms of the boost converter for  $D = 0.5$ .

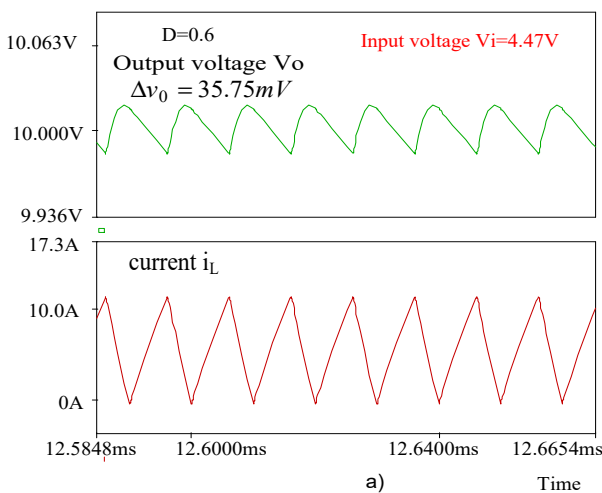
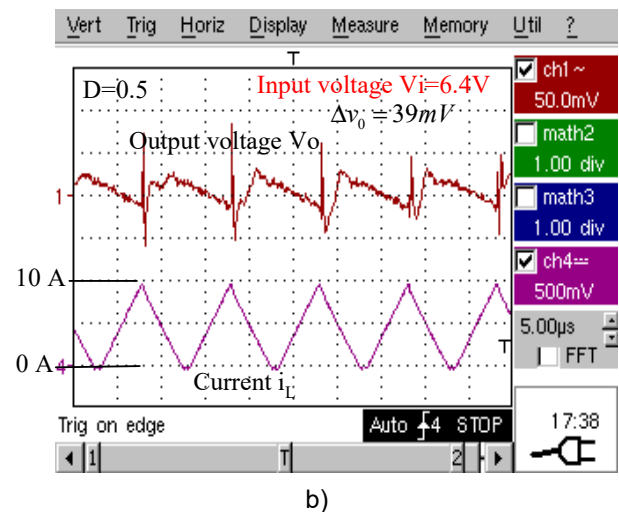


**Figure 14.** (a) Simulated waveforms of the boost converter for  $D = 0.6$ . (b) Experimental waveforms of the boost converter for  $D = 0.6$ .

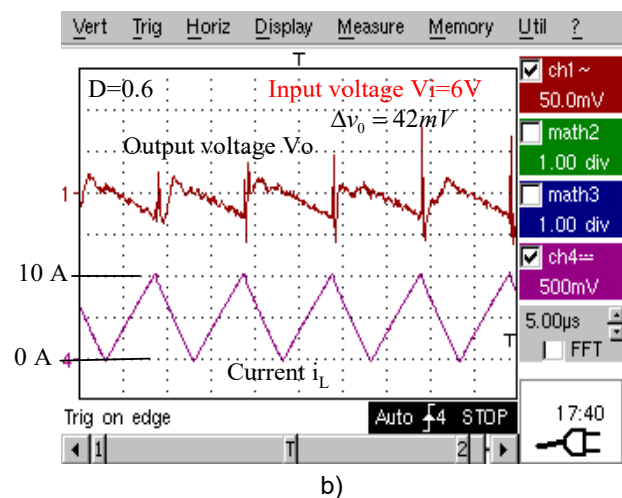
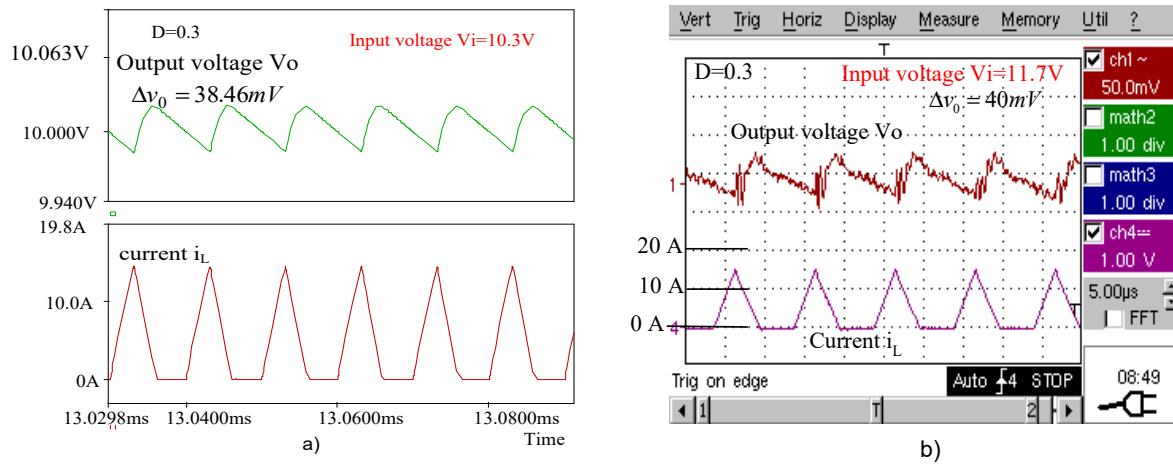
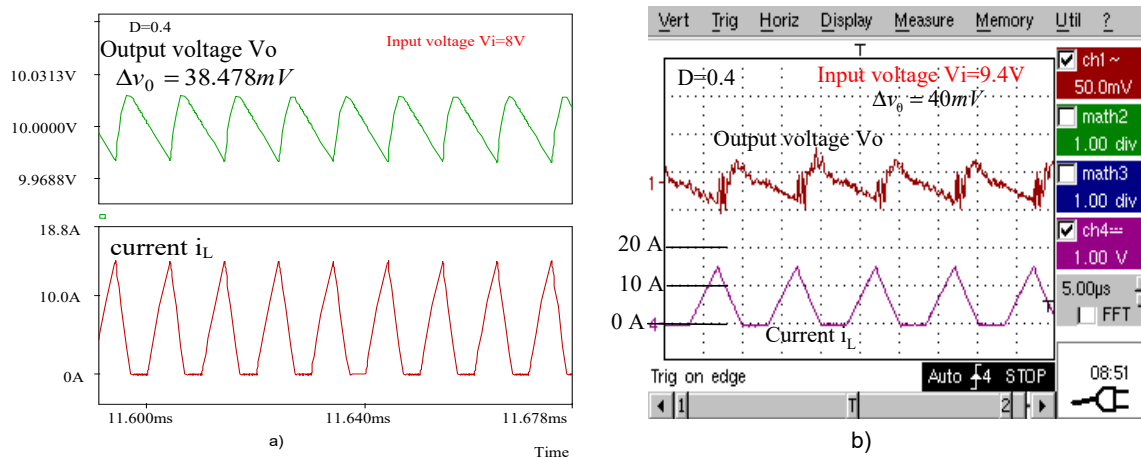


Figure 15a,b present the waveforms of the output voltage  $v_o$  and inductor current  $i_L$  obtained for the buck–boost converter by simulation and by experimental tests, respectively, when operating with a duty cycle  $D = 0.3$ . The same waveforms are given in Figure 16a,b for  $D = 0.4$ , in Figure 17a,b for  $D = 0.5$ , and in Figure 18a,b for  $D = 0.6$ .



**Figure 15.** (a) Simulated waveforms of the buck–boost converter for  $D = 0.3$ . (b) Experimental waveforms of the buck–boost converter for  $D = 0.3$ .



**Figure 16.** (a) Simulated waveforms of the buck–boost converter for  $D = 0.4$ . (b) Experimental waveforms of the buck–boost converter for  $D = 0.4$ .

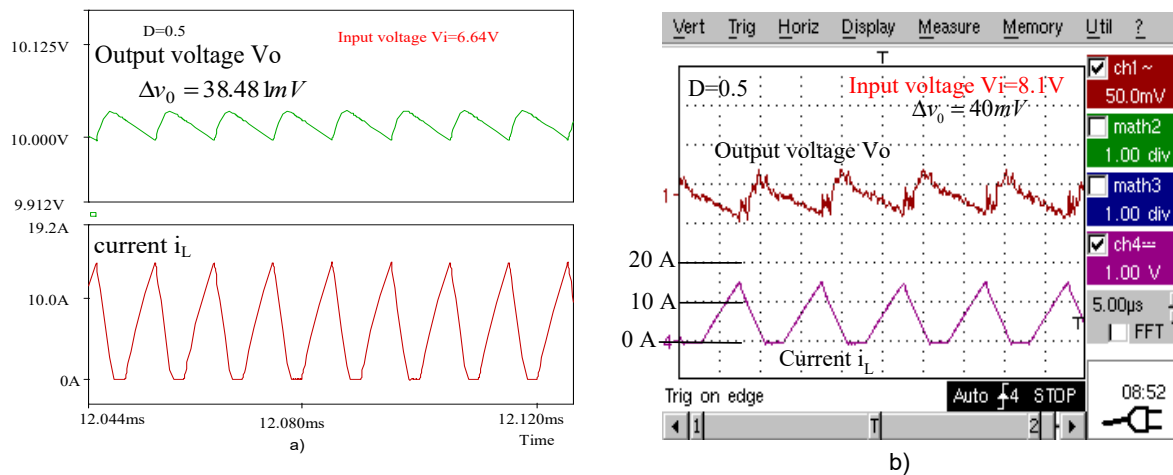


**Figure 17.** (a) Simulated waveforms of the buck–boost converter for  $D = 0.5$ . (b) Experimental waveforms of the buck–boost converter for  $D = 0.5$ .



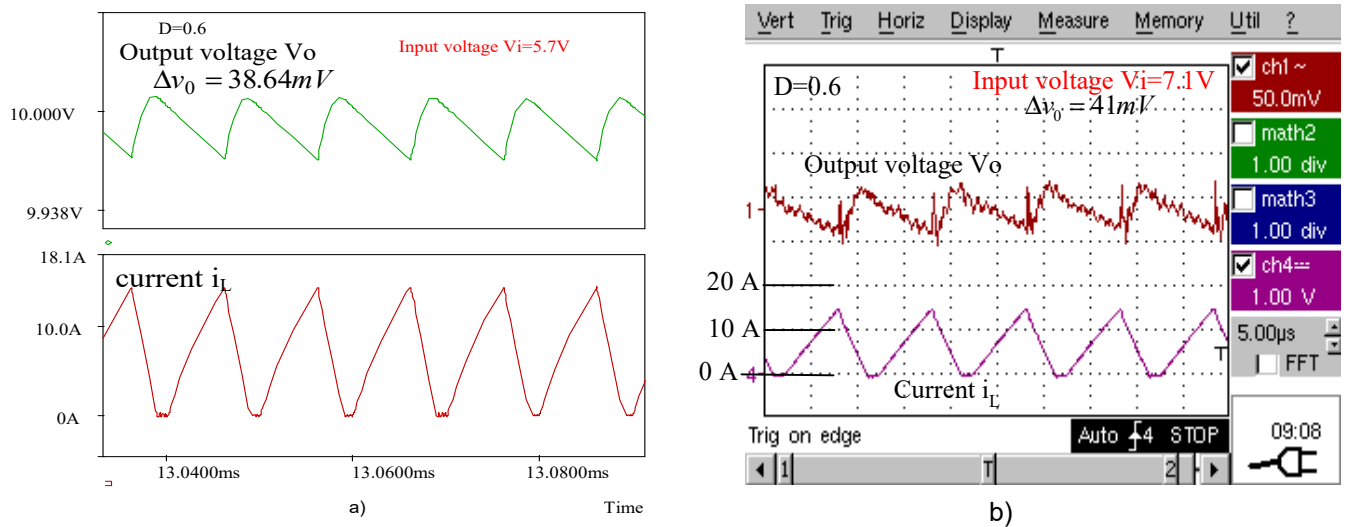


**Figure 18.** (a) Simulated waveforms of the buck–boost converter for  $D = 0.6$ . (b) Experimental waveforms of the buck–boost converter for  $D = 0.6$ .

The peak-to-peak voltage ripples of the buck–boost converter output are presented in Table 7. The experimental values are compared with those calculated using the novel expressions and with the simulated ones.

**Table 7.** Peak-to-peak voltage ripples at the buck–boost converter output.

Duty Cycle	30%	40%	50%	60%
$\Delta V_o$ experiment	40 mV	40 mV	40 mV	41 mV
$\Delta V_o$ calculated	39.846 mV	39.846 mV	39.846 mV	39.846 mV
$\Delta V_o$ simulated	38.46 mV	38.478 mV	38.48 mV	38.64 mV

## 6. Conclusions

This paper examines the voltage ripple at the output of DC converters, including the ripple observed during operation in DCM, for which new calculation formulas were derived. For the boost and buck–boost converters, improved formulas are provided to enhance ripple estimation, especially during CCM operation at duty cycles near the transition point between CCM and DCM. This study demonstrates that these new formulas diverge from commonly used ones when the boundary duty cycles are less than or equal to 0.5.

In sources where converters operate in DCM mode, the output voltage depends not only on the duty cycle but also on the load resistance. Consequently, if the sources are regulated and the load resistance varies significantly, the converters will function across a wide range of duty cycles. Therefore, the derived formulas were validated for duty cycle values ranging from 0.3 to 0.6.

The ripple values obtained through calculations and simulations are closely aligned. As anticipated, the values measured in experimental tests are higher, since the derived formulas are based on ideal converter models. Nevertheless, these formulas are still effective for prototype design, with the final output capacitance values being determined through experimental validation.

These novel expressions also provide valuable insights for the design process. First, when a buck converter operates in DCM as opposed to CCM, the inductance value has a minimal impact on the peak-to-peak ripple normalized to the average output voltage.



Second, in the case of the buck–boost converter (and consequently the flyback converter), this normalized ripple is independent of the duty cycle.

The derived equations demonstrate that, across all operating modes and for all converters, the normalized ripple relative to the average output voltage is inversely proportional to the value of the output capacitance. These relationships can be employed either to calculate the normalized ripple, given the known component values of the converter, or to determine the required output capacitance to achieve a specified normalized ripple.

Additionally, these relations enable a straightforward assessment of how variations in specific component values—potentially within a broad range—affect the normalized ripple, thereby facilitating optimization efforts.

**Author Contributions:** Conceptualization, N.L. and M.L.; methodology, N.L., M.L., C.A. and O.U.; validation, N.L., M.L., C.A. and O.U.; writing—original draft preparation, N.L., M.L., C.A. and O.U.; writing—review and editing, N.L., M.L., C.A. and O.U. All authors have read and agreed to the published version of the manuscript.

**Funding:** This research received no external funding.

**Data Availability Statement:** The raw data supporting the conclusions of this article will be made available by the authors on request.

**Conflicts of Interest:** The authors declare no conflict of interest.

## References

1. Erickson, R.W.; Maksimovic, D. *Fundamental of Power Electronics*, 2nd ed.; Kluwer Academic Publishers: Dordrecht, The Netherlands, 2001.
2. Rashid, M.H. *Power Electronics Handbook*; Elsevier: Amsterdam, The Netherlands, 2018.
3. Lucanu, M.; Lucanu, N.; Ursaru, O. *Convertoare de Current Continuu Pentru Surse în Comutație*; PIM: Iasi, Romania, 2021; ISBN 978-606-13-6549-4.
4. Moschopoulos, G. *DC-DC Converter Topologies: Basic to Advanced*; Wiley-IEEE Press: Hoboken, NJ, USA, 2023; ISBN 978-1-119-61242-1.
5. Wei, C.L.; Shih, M.H. Design of a switched-capacitor DC-DC converter with a wide input voltage range. *IEEE Trans. Circuits Syst.* **2013**, *60*, 1648–1656. [[CrossRef](#)]
6. Duong, T.D.; Nguyen, M.K.; Tran, T.T.; Lim, Y.C.; Choi, J.H. Transformerless high step-up DC-DC converters with switched-capacitor network. *Electronics* **2019**, *8*, 1420. [[CrossRef](#)]
7. Durán, E.; Litrán, S.P.; Ferrera, M.B. Configurations of DC–DC converters of one input and multiple outputs without transformer. *IET Power Electron.* **2020**, *13*, 2658–2670. [[CrossRef](#)]
8. Melo de Andrade, J.; Coelho, R.F.; Lazzarin, T.B. High step-up dc–dc converter based on modified active switched-inductor and switched-capacitor cells. *IET Power Electron.* **2020**, *13*, 3127–3137. [[CrossRef](#)]
9. Sayed, K.; Almutairi, A.; Albagami, N.; Alrumayh, O.; Abo-Khalil, A.G.; Saleeb, H. A review of DC-AC converters for electric vehicle applications. *Energies* **2022**, *15*, 1241. [[CrossRef](#)]
10. Algamluoli, A.F.; Wu, X.; Mahmood, M.F. Optimized DC–DC converter based on new interleaved switched inductor capacitor for verifying high voltage gain in renewable energy applications. *Sci. Rep.* **2023**, *13*, 16436. [[CrossRef](#)] [[PubMed](#)]
11. Zhang, X.; Wang, T.; Bao, H.; Hu, Y.; Bao, B. Stability Effect of Load Converter on Source Converter in a Cascaded Buck Converter. *IEEE Trans. Power Electron.* **2023**, *38*, 604–618. [[CrossRef](#)]
12. Biela, J.; Badstuebner, U.; Kolar, J.W. Impact of Power Density Maximization on Efficiency of DC–DC Converter Systems. *IEEE Trans. Power Electron.* **2009**, *24*, 288–300. [[CrossRef](#)]
13. Forouzesh, M.; Siwakoti, Y.P.; Gorji, S.A.; Blaabjerg, F.; Lehman, B. Step-Up DC-DC Converters: A Comprehensive Review of Voltage-Boosting Techniques, Topologies, and Applications. *IEEE Trans. Power Electron.* **2017**, *32*, 9143–9178. [[CrossRef](#)]
14. He, W.; Ortega, R. Design and Implementation of Adaptive Energy Shaping Control for DC–DC Converters With Constant Power Loads. *IEEE Trans. Ind. Inform.* **2019**, *16*, 5053–5064. [[CrossRef](#)]
15. Bao, D.; Kumar, A.; Pan, X.; Xiong, X.; Beig, A.R.; Singh, S.K. Switched inductor double switch high gain DC-DC converter for renewable applications. *IEEE Access* **2021**, *9*, 14259–14270. [[CrossRef](#)]
16. Aravind, R.; Bharatiraja, C.; Verma, R.; Aruchamy, S.; Mihet-Popa, L. Multi-Port Non-Isolated DC-DC Converters and their Control Techniques for the Applications of Renewable Energy. *IEEE Access* **2024**, *12*, 88458–88491. [[CrossRef](#)]
17. Górecki, P.; Górecki, K. Methods of Fast Analysis of DC–DC Converters—A Review. *Electronics* **2021**, *10*, 2920. [[CrossRef](#)]

18. Liu, S.-L.; Liu, J.; Mao, H.; Zhang, Y.-Q. Analysis of operating modes and output voltage ripple of dc-dc converters and its design considerations. *IEEE Trans. Power Electron.* **2008**, *23*, 1813–1821. [[CrossRef](#)]
19. Liu, S.-L.; Li, Y.; Liu, L. Analysis of output voltage ripple of buck dc-dc converter and its design. In Proceedings of the 2009 2nd International Conference on Power Electronics and Intelligent Transportation System (PEITS), Shenzhen, China, 19–20 December 2009; Volume 2, pp. 112–115.
20. Babaei, E.; Mahmoodieh, M.E.S.; Mahery, H.M. Operational modes and output-voltage-ripple analysis and design considerations of buck-boost dc-dc converters. *IEEE Trans. Ind. Electron.* **2012**, *59*, 381–391. [[CrossRef](#)]
21. Billings, K.; Morey, T. *Switchmode Mode Power Supply Handboock*, 3rd ed.; Mc. Graw Hill: New York, NY, USA, 2011.
22. Deraz, S.A.; Zaky, M.S.; Tawfiq, K.B.; Mansour, A.S. State Space Average Modeling, Small Signal Analysis, and Control Implementation of an Efficient Single-Switch High-Gain Multicell Boost DC-DC Converter with Low Voltage Stress. *Electronics* **2024**, *13*, 3264. [[CrossRef](#)]
23. Vitale, G.; Lullo, G.; Scire, D. Thermal Stability of a DC/DC Converter with Inductor in Partial Saturation. *IEEE Trans. Ind. Electron.* **2021**, *68*, 7985–7995. [[CrossRef](#)]

**Disclaimer/Publisher’s Note:** The statements, opinions and data contained in all publications are solely those of the individual author(s) and contributor(s) and not of MDPI and/or the editor(s). MDPI and/or the editor(s) disclaim responsibility for any injury to people or property resulting from any ideas, methods, instructions or products referred to in the content.